

сообщения
объединенного
института
ядерных
исследований
дубна

E4-84-487

P.Mädler, P.Yu.Nikishov, B.N.Zakhariev

**INTENSIFIED AND ASYMMETRIC
BARRIER PENETRATION
OF NUCLEAR SLABS
IN TDHF APPROXIMATION**

1984

1. Introduction

Quantum tunnelling phenomena are of fundamental interest for the understanding of a variety of processes in the microworld (decay of quasistationary states, nuclear reactions with sub-barrier particle emission, sub-barrier fusion, spontaneous fissions, etc.) as well as for a lot of its practical applications (Josephson effect, highest-precision investigations of solid-body surfaces within an accuracy smaller than atomic diameters^{/1/}, etc.).

The behaviour of a single (elementary) quantum mechanical particle in an external potential field was widely understood still at the beginning of the development of quantum mechanics. Nevertheless, presently, investigations are going on of several special situations leading to qualitatively new and partially surprising results. For example, we mention penetration through singular potentials which are nonpenetrable in the quasiclassical approximation^{/2/}; resonance-like penetrability of a potential composed of 2 δ -functions at finite distance^{/3/}; and the existence of bound states with positive energies for potential wells whose tails show a damped oscillating behaviour (the bound state may lie even above the oscillating part), which is due to multiple reflection above the barrier^{/4/}.

Up to now, there are only a very few investigations concerning barrier penetration of complex particles exhibiting intrinsic degrees of freedom (e.g., nuclei). Frequently, in such type of problems the inner structure of the particle is completely neglected.

On the other hand, it could be shown^{/5,6/} that in the case that intrinsic excitations can be excluded (existence of a gap between ground state and first excited state and comparable small energies of the center of mass motion), the tunnelling of a complex particle through an external barrier can be essentially intensified if taking into account the mutual intrinsic motion of the particles in the ground state of the complex.

Another very interesting result is the finding of ref.^{/7/} that in the case when intrinsic excitation is possible, the penetrability of an asymmetric external potential for a complex particle can show a very pronounced left to right asymmetry (at the same energy of the incoming particle).



These results have been obtained either in a rather schematic way or by using several simplifying assumptions to consider a one-dimensional pair of particles interacting via an infinite rectangular potential colliding with an external rectangular barrier.

Owing to the large number of practical consequences of the above-mentioned effects a more involved consideration should, therefore, be of interest.

The aim of the present paper is to analyse in TDHF approximation the behaviour of (effectively) one-dimensional nuclear slabs of different thickness (particle number per unit area) when interacting with asymmetric as well as symmetric external potentials and to compare the results with those of refs.^{/5-7/}.

2. Qualitative Considerations

We start with a brief description of the basic ideas of refs.^{/5-7/}.

First, consider the penetration of an external barrier $V(x)$ by two identical elementary particles. In WKB approximation the transmission coefficient $D(E)$ is given by

$$D(E) \sim \exp \left[-\frac{1}{\hbar} \int_a^b \sqrt{2m(V(x) - E)} dx \right]. \quad (1)$$

From eq. (1) it is obvious that the transmission coefficients are exactly the same for the case when the two particles are considered to form a complex and the intrinsic motion is fully neglected, and for the case of independent penetration of both particles simultaneously. In the first case one has to double m , $V(x)$, E , and in the second to square eq. (1) ending up with $D^2(E)$ in both extreme limits (in general, however, this is only exact in the quasiclassical case).

Turning to some intermediate situation of the two particles initially being bound in the ground state of the complex Φ_0 , we decompose the wave function of the system with respect to the full set of intrinsic wave functions Φ_α

$$\Psi(x_1, x_2) = \sum_{\alpha} F_{\alpha}(R) \Phi_{\alpha}(\rho) \quad (2)$$

with $R = (x_1 + x_2)/2$, $\rho = x_2 - x_1$.

If the energy of the incoming complex particle is smaller than the energy of the first excited state, one can neglect all terms with $\alpha > 0$ in eq. (2). Then, for the wave function $F_0(R)$, describing the motion of the complex as a whole, one ends up with the Schrödinger equation^{/6/}

$$-\frac{\hbar^2}{2M} F_0''(R) + V_{00}(R) F_0(R) = E F_0(R), \quad M = 2m \quad (3)$$

with the effective potential felt by the complex particle

$$V_{00}(R) = \int |\Phi_0(\rho)|^2 [V(R - \frac{1}{2}\rho) + V(R + \frac{1}{2}\rho)] d\rho \quad (4)$$

which appears to be the external potential for both constituents averaged over the intrinsic motion.

Using the normalization condition for Φ_0 it is easy to show that

$$\int V_{00}(R) dR = 2 \int V(R) dR. \quad (5)$$

If the pair of particles is much smaller than the half width of the potential, $V_{00}(R)$ approaches $2V(R)$, i.e., it feels twice the potential of each of its constituents. A reduction of the barrier height in a more realistic case can drastically enlarge penetrability for not too small incident energies (the corresponding broadening of the effective barrier can, however, diminish penetrability at very small energies). This is the essence of the "intensified tunnel effect"^{/5/}.

Consider now an asymmetric potential exhibiting a steep fall off on the one side and a flatter one on the other side. It can be shown^{/7/} that its penetrability for the two-particle complex is exactly the same for approaching the barrier from any of the sides if real excitations can be excluded. However, if other channels come into play and the corresponding terms are retained in eq. (2), the transmission coefficient is larger for approaching the barrier from the flat side. It is argued^{/7/} that this is because the complex particle becomes less excited in this case and, consequently, more kinetic energy remains to tunnel through the barrier with a higher probability. Considering only the ground and first excited states, numerical calculations have been performed for a one-dimensional pair of particles interacting via an infinite rectangular potential and colliding with an asymmetric step potential. The results confirmed the above qualitative expectations.

It is of great interest to consider analogous problems for a complex of $N > 2$ particles. Intuitively one could claim that the intensified tunnel effect will increase with increasing particle number since more and more intrinsic degrees of freedom "help" the system to "adapt" itself to an external barrier and to collectively overcome it. On the other hand, with increasing particle number the excited states come down in energy and the spectrum of states becomes more dense. Hence, the neglect of intrinsic excitations becomes less motivated: since intrinsic excitations decrease the kinetic energy of the system, the barrier should become less penetrable.

To get a reasonable guess about the N -dependence of the asymmetry effect is possibly even more difficult. We have the feeling that for a given degree of the potential asymmetry it could be most pronounced for systems of diameters comparable with the thickness of the potential. For a given particle number in the complex it seems to us that the effect should increase with increasing potential asymmetry. Exact investigations on this line are, however, in order.

In a quantitative N -particle description of the two collective barrier penetration effects, it is desirable to include also dynamical deformations as well as break-up and fragmentation channels which may play an essential role in the given problem and have not been investigated explicitly in refs.^{/5-7/} (e.g., break-up of a deuteron when colliding with the external barrier).

Since the exact N -particle Schrödinger equation for the given problem cannot be solved exactly we treat it in the standard TDHF approximation with effective nucleon-nucleon interactions^{/8-12/}. In TDHF the wave function is described by a Slater determinant specified by the criterion that at every time, the deviation between it and the exact solution of the Schrödinger equation is minimized. The corresponding variation principle yields a nonlinear system of coupled single-particle Schrödinger equations for each initially occupied orbital, and, therefore, is much more easier to handle than the exact problem. However, due to the nonlinearity of the equations the superposition principle of exact (linear) quantum mechanics is lost. This has a lot of consequences^{/8-12/} like some classical (deterministic) features of the TDHF solutions, the existence of soliton-like solutions, spurious asymptotic cross channel correlations, and corresponding fundamental questions of the interpretation of numerical results. We should have these specific features which are the price for the drastic reduction of the full problem in mind for the interpretation of the barrier penetration results presented below. Here, we mention in passing that no problems with interpretation arise if one is satisfied with expectation values of one-body operators (e.g., mean particle number transmitted or reflected in the given problem) instead of trying to look for specific channels, i.e. S -matrix elements.

For simplicity of numerical calculations we restrict ourselves to the considerations of an effective one-dimensional slab geometry.

3. Model and Slab Characteristics

We perform our investigations of barrier penetration in the framework of the simple, effectively one-dimensional, model for nuclear

slabs proposed in ref.^{/8/}. In this geometry the slab has a finite dimension in the z -direction and is translationally invariant in directions perpendicular to the z -axis. So, the single-particle wave functions are of the form

$$\Psi_{n\vec{k}_\perp}(\vec{r}, t) = \Omega^{-\frac{1}{2}} \exp[i(\vec{k}_\perp \vec{r}_\perp - \hbar k_\perp^2 t / 2m)] \phi_n(z, t) \quad (6)$$

and with the effective nucleon-nucleon interaction chosen to be a simplified Skyrme force

$$V(\vec{r}_1, \vec{r}_2) = (t_0 + \frac{1}{2}t_3 \rho) \delta(\vec{r}_1 - \vec{r}_2) \quad (7)$$

with $t_0 = -1090$ MeV fm³, $t_3 = 17288$ MeV fm⁶, and ρ being the one-body density

$$\rho(\vec{r}, t) \equiv \rho(z, t) = \sum_{n=1}^N a_n |\phi_n(z, t)|^2 \quad (8)$$

we have to solve numerically a coupled system of one-dimensional Schrödinger-type equations for the evolution of the single-particle orbitals ϕ_n occupied in the initial state:

$$i\hbar \dot{\phi}_n(z, t) = \left[-\frac{\hbar^2}{2m} \frac{\partial^2}{\partial z^2} + \frac{3}{4} t_0 \rho(z, t) + \frac{3}{16} t_3 \rho^2(z, t) + V(z) \right] \phi_n. \quad (9)$$

Here V denotes the external potential. The (constant) occupation numbers a_n monotonically decrease with increasing n expressing the fact that for higher orbitals less plane waves fulfill the condition

$$|\vec{k}_\perp| \leq [(2m/\hbar^2)(\epsilon_F - \epsilon_n)]^{1/2} \equiv k_{max}(n). \quad (10)$$

So, higher orbitals enter the density with smaller weights than lower ones.

Initial conditions are constructed from stationary solutions of eq. (9) (with $V(z) \equiv 0$) boosted into direction of the external barrier by multiplying with plane waves corresponding to the given kinetic energy of the slab (for details see^{/8/}).

The Pauli principle has been built in from the beginning and is satisfied at all times simply because all the particles are moving in the same potential^{/8/}.

Since in the following we shall investigate slabs of different thickness \mathcal{A}

$$\mathcal{A} = \sum_{n=1}^N a_n, \quad a_n = k_{max}^2(n) / \pi, \quad (11)$$

it is useful to illustrate the corresponding stationary solutions. Fig. 1 shows the \mathcal{A} -dependence of single-particle energies ϵ_n , the Fermi energy ϵ_F and the number of occupied discrete states N . Note, that our slab mass table slightly deviates from that of ref.^{/8/} since in that work an additional finite range Yukawa interaction in the

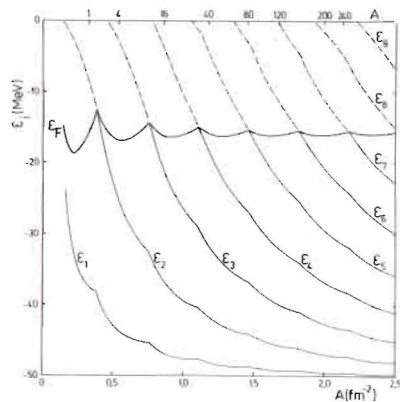


Fig. 1. The slab mass table for the effective force of eq. (7). The A -dependence of the single-particle energies ϵ_n (solid lines - occupied, dashed lines - unoccupied levels) and the Fermi energy ϵ_F (heavy line) is shown. The upper abscissa is labeled by the three-dimensional equivalent mass number determined from $A = 2 r_0 A^{1/3} \rho_0$.

effective force, eq. (7), has been considered. "Magic" slabs occur when a new eigenvalue dives below ϵ_F . The nearly equidistant "shells" have a distance of

$$\Delta A \approx 0.36 \text{ fm}^{-2}, \quad (12)$$

while the first "magic" slab has a thickness of $A = 0.39 \text{ fm}^{-2}$. In using the notions "shells" and "magic" slabs one should, however, have in mind that translational invariance in the transverse directions gives rise to a continuous spectrum, so that no gaps in the single-particle spectrum appear^{13/}. Nevertheless, one can expect that "magic" slabs are to some extent distinguished in a dynamical evolution since the continuous transverse degrees of freedom are frozen. As could be expected, the Fermi energy oscillates around the nuclear matter value for the energy per nucleon $\epsilon_0 = -16 \text{ MeV}$.

The numerical method used to solve eq. (9) is a finite-series expansion of the evolution operator with the mean-field Hamiltonian h taken at half time step

$$\phi_n(t+\Delta t) \approx \sum_{j=0}^J \frac{1}{j!} \left[-\frac{1}{\hbar} \Delta t \left\{ h\left(t+\frac{1}{2}\Delta t\right) + V \right\} \right]^j \phi_n(t). \quad (13)$$

Numerical stable results could mostly be achieved for a spatial step size of $\Delta z = 0.5 \text{ fm}$, a length of the numerical box $L = 100 \text{ fm}$, and $J = 4$ (for a discussion of numerical stability, with respect to slab collisions, see also ref.^{13/}). An exception was the energy region around the first discontinuity of the transmission probability (see below). In this case J has been substantially enlarged in order to decrease the degree of nonunitarity of the approximate evolution operator in eq. (13) characterized by eigenvalues greater than or equal to 1 and causing exponential amplifications of the wave functions and corresponding strong violation of norm and energy conservation. In fact,

such type of instabilities cannot be fully excluded in this way; we rather have shifted the time of their onset to a later instant, out of the time interval of interest.

In connection with numerical stability it is interesting to point out that, while in slab collisions the evolution of the main parts of the density profiles ($\rho \gtrsim 0.1 \rho_0$) comes close to the stable results already at step sizes of about $\Delta z = 1 \text{ fm}$ and only the small-density tails ("promptly emitted particles" - PEP) are drastically different from the stable shapes (reached at about $\Delta z = 0.5 \text{ fm}$), in the given connection of barrier penetrations the evolution of the density profiles at all and, hence, the transmission coefficients reach stability only for $\Delta z \lesssim 0.5 \text{ fm}$. For a step size of $\Delta z = 1 \text{ fm}$ the dependence of the transmission coefficient $D(E)$ on energy per particle E (for a given potential V and slab thickness A) is qualitatively similar in shape. The essential difference is that for the same value of D roughly twice the energy is required as compared to the stable case. Furthermore, the curve $D(E)$ exhibits small stochastic ripples obviously being connected with insufficient numerical accuracy and disappearing with decreasing Δz .

4. Numerical Results and Discussions

A detailed investigation of intensified and asymmetric barrier penetration in the present model would require to independently vary barrier height, the degree of asymmetry of the potential, slab thickness, and slab incident energy. For each combination of these quantities a full TDHF evolution according to eq. (9) would have to be performed. To limit the number of necessary calculations we restrict ourselves to the consideration of an asymmetric Gaussian

$$V(z) = V_0 \begin{cases} \exp(-z^2/2a_1^2) & , z \geq 0 \\ \exp(-z^2/2a_2^2) & , z \leq 0 \end{cases} \quad (14)$$

with $V_0 = 10 \text{ MeV}$, $a_1 = 1.5 \text{ fm}$, $a_2 = 3.5 \text{ fm}$, and consider its penetrability for slabs of thickness $A = 2.0, 1.0, 0.8, 0.75, 0.3 \text{ fm}^{-2}$ and incident energies per particle in sufficiently small steps (in order to get smooth curves for $D(E)$ through the calculated points) ranging from values for which $D(E) = 0$ up to energies for which $D(E) = 1$. All these calculations have been done for approaching the potential from the steep side as well as from the flat side. Additionally the same calculations have been performed for the symmetric Gaussian potential $a_1 = a_2 = 2.5 \text{ fm}$ (with unchanged V_0) in order to compare with the asymmetric results.

It is known that single-particle effects play a crucial role in TDHF nuclear dynamics^{/8-12/}. Minute changes in initial conditions may easily result in qualitative changes in the nature of the considered reaction. Therefore, we start our presentation of numerical results with the discussion of the time evolution of individual single particle wave packets and its relation to the barrier penetration process of the slab. In Fig. 2 full as well as partial densities are displayed for an illustrative example.

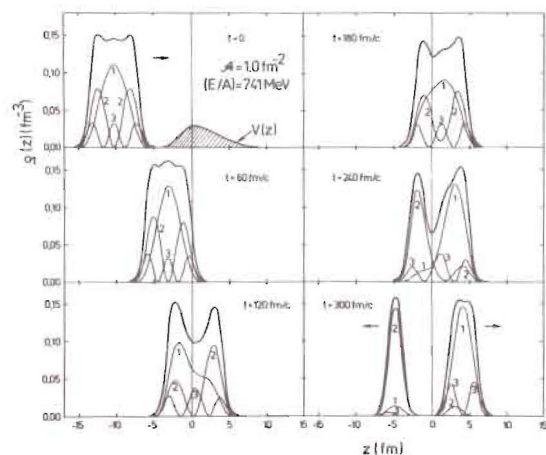


Fig. 2. Contributions of individual single particle orbitals $a_n |\phi_n|^2$ (thin lines, marked by a corresponding number $n=1,2,3$) to the full density $\rho(z)$ (heavy lines) at various times for a $\mathcal{A}=1.0 \text{ fm}^{-2}$ slab colliding with the potential eq. (14) from the steep side at $E/A = 7.41 \text{ MeV}$. For $t=0$ the external barrier is also shown (hatched region) in arbitrary units. The position of the maximum ($z=0$) of the potential is marked by a vertical thin line.

In the given case only 3 orbitals are occupied (compare Fig. 1). After having solved the TDHF equations (9) each single particle wave packet can be independently considered as moving in the (given) time-dependent mean potential^{/8/}. The wave functions ϕ_n may be decomposed into Fourier components, the dominant velocities being

$$V_n^\pm = V_0 \pm \left[\frac{2}{m} (\epsilon_n - W) \right]^{1/2},$$

where V_0 is the initial velocity of the slab, ϵ_n is the static eigenvalue of ϕ_n and W is the average well depth which is initially -50.3 MeV in the given case. For qualitative discussions we omit the time dependence of W in the following. The velocities V_n^\pm , V_0 , and the velocity V_b which a classical particle needs to overcome the barrier (10 MeV) are:

$$\begin{aligned} V_1^+ &= 0.202 \text{ c}, & V_1^- &= 0.05 \text{ c} \\ V_2^+ &= 0.279 \text{ c}, & V_2^- &= -0.027 \text{ c} \\ V_3^+ &= 0.351 \text{ c}, & V_3^- &= -0.099 \text{ c} \\ V_0 &= 0.126 \text{ c}, & V_b &= 0.146 \text{ c}. \end{aligned}$$

In restricting discussion to the dominant components V_n^\pm one should have in mind that the Fourier decomposition of ϕ_n really yields a velocity distribution around V_n^\pm . The V_1^+ component has sufficient velocity to overcome the barrier while V_1^- being positive (i.e., also moving towards the barrier) is substantially smaller than V_b and, therefore, is reflected from it. This leads to the significant deformation of the first orbital at $t = 120 \text{ fm/c}$. Shortly after, the V_1^- component is reflected from the backward edge of the mean field potential well which moves with V_b and, hence, acquires velocity V_1^+ which enables it to overcome the barrier. At $t \gg 180 \text{ fm/c}$ it is really seen that a large fraction of the first orbital is beyond the top of the barrier. The small fraction which could not overcome the barrier corresponds to the small-velocity components in the tail of the distribution of the Fourier components. The second orbital begins to "feel" the barrier at an earlier instant since it is closer to the surface of the slab. Hence, a slight deformation can be stated already at $t = 60 \text{ fm/c}$. It is, however, caused only by the reflection of a small amount of velocity components from the barrier since $V_2^+ > V_b$ and $V_2^- < 0$ (i.e., moves away from the barrier). So, the second orbital moves first to the backward edge of the slab, then to the opposite edge being mainly concentrated at $z < 0$ for $t = 240 \text{ fm/c}$ when the first orbital is at $z > 0$. A deep minimum in the total density, consequently, arises connected with a corresponding barrier in the self-consistent mean potential suppressing free motion of the orbitals in the whole slab. In the given situation the repulsive external potential dominates the attractive nuclear force between the two halves of the slab, so that it becomes partly reflected and transmitted. The third orbital is even less deformed than the second and its weight in the total density (mean field) is quite small. So, the fractions of it, which are finally trapped in the reflected and transmitted fragments, are mainly determined by the evolution of the first and second orbitals.

To illustrate the delicate interplay between repulsive external potential and attractive nuclear force, we consider now a thick ($\mathcal{A} = 2.0 \text{ fm}^{-2}$) slab colliding with the same potential as in the above case at two quite close incident energies (8.56, 8.62 MeV/A). Fig. 3 shows the corresponding density profiles and velocity distributions

$$V(z,t) = \frac{1}{\rho(z,t)} \frac{\hbar}{m} \sum_{n=1}^N a_n \text{Im} \left(\phi_n^* \frac{\partial}{\partial z} \phi_n \right) \quad (15)$$

at several times. Note, that in the initial state from (15) follows $V(z,t=0) \equiv V_0$ as it should. For both incident energies the evolution of the system is nearly the same with respect to both density and velocities. In both cases at about $t = 120 \text{ fm/c}$ a deep minimum of the

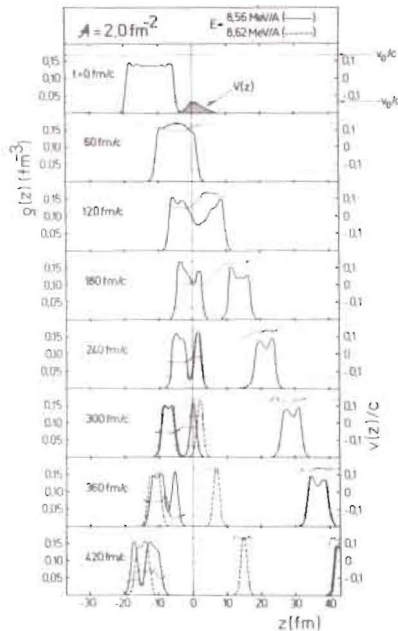


Fig. 3. Density profiles (heavy lines) at several times for a slab of thickness $A = 2.0 \text{ fm}^{-2}$ colliding with the same potential as in Fig. 2 at incident energy 8.56 MeV/A (full lines) and 8.62 MeV/A (dashed lines). The vertical thin line marks the position of the potential barrier while the two horizontal thin lines denote the incident velocity v_0/c which the slab would have in the absence of the barrier, and $-v_0/c$ for an elastic reflection. The scale to the right concerns velocities (in units of c) while the left-hand scale corresponds to the density.

density appears at $z > 0$ leading to the transmission of a first fragment while the remaining part of the slab still stands on the top of the barrier. At about $t = 240 \text{ fm}/c$ a further deep minimum arises at $z < 0$. At the higher energy it is slightly closer to

$z = 0$. The right-hand part of the fragment has slightly larger velocities than for the lower energy case, although in both cases its velocities are negative. So, it seems at $t = 240 \text{ fm}/c$ as if the remaining fragment becomes reflected as a whole. At later instants, however, it becomes clear, that this happens only for the lower incident energy while at the higher energy part of this fragment is transmitted. It is quite surprising that not only the first transmitted fragment but also the second one have velocities close to v_0 .

Substantial oscillations of the density for large times indicate that part of the initial kinetic energy is converted into internal excitations. In the example shown in Fig. 3 the excitation energy amounts to 41%, and in that of Fig. 2 to 26% of the total energy of the system. Since in both cases the incident energies are approximately the same and the same barrier has been considered, one can conclude that the degree of excitation decreases with decreasing slab thickness, i.e., decreasing number of occupied orbitals. For a very thin slab of $A = 0.3 \text{ fm}^{-2}$ (one orbital occupied) at the same incident energy only 2.2% of the total energy go into excitation.

We turn now to the discussion of the energy dependence of the transmission coefficient $D(E)$ for slabs of different thickness. We

determine this quantity by simply counting the particle number at $z > 0$ at large t , i.e.,

$$D(E) = \frac{1}{A} \int_0^{\infty} \rho_E(z, t \rightarrow \infty) dz. \quad (16)$$

We mention in passing that eq. (16) is not an exact definition in the sense of time-dependent scattering theory. In principle, the definition of $D(E)$ should contain the integral of the diagonal part of the N -particle density matrix at $t \rightarrow \infty$ over $z_N > 0$ for each coordinate z_1, \dots, z_N . Although in TDHF approximation the N -particle density matrix at any time reduces to the antisymmetrized product of one-particle density matrices $\rho_E(z_n)$, the N -fold integral over $z_N > 0$ does not reduce to eq. (16) since the single-particle functions ϕ_n are not orthonormal in the right half-space (the discussion of Fig. 2 has shown that asymptotically any orbital has components as to the right as well as to the left). However, due to the well-known artifact of that standard TDHF theory⁸⁻¹² called "asymptotic cross channel correlations", a more exact expression for $D(E)$ would not exist in the sense that it would continue to depend on time even for $t \rightarrow \infty$. Therefore, in accordance with the aim of TDHF to optimally describe expectation values of one-body operators (particle number operator in the right half-space, in the given case) we use the more "classical" definition of eq. (16).

For a slab of $A = 1.0 \text{ fm}^{-2}$ colliding with potential (14) from the steep side the transmission coefficient D is shown in Fig. 4 as a function of energy. The somewhat unexpected result is that it is different from zero and unity only in a very small energy interval (below the barrier height V_0). At $E = E_1 = 7.315 \text{ MeV}$ it immediately jumps from zero to about $D = 0.6$. Then, with further slight enlargement of E it slightly increases to about $D = 0.65$ at $E_2 = 7.492 \text{ MeV}$ where it has a second discontinuity and acquires unity value for $E > E_2$. The

case of $E = 7.41 \text{ MeV}$ lying in between E_1 and E_2 was already discussed (Fig. 2).

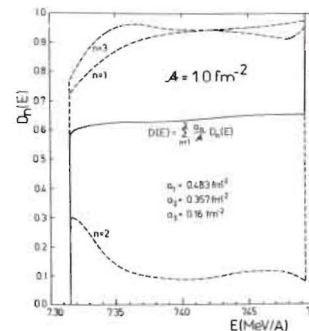


Fig. 4. Total (full line) and partial transmission coefficients (dashed lines marked by the number of the corresponding orbital) for a slab of thickness $A = 1.0 \text{ fm}^{-2}$ colliding with potential (14) from the steep side as functions of incident energy.

The E -dependence of the partial transmission coefficients $D_n(E)$ (percentage of the n -th orbital being transmitted) near the discontinuities indicates that they are not caused by discontinuities in the behaviour of single orbitals. Indeed, at any energy from 7 to 8 MeV a deep minimum of the density arises (as shown in Fig. 2) in the vicinity of the position of the barrier top. For $E < E_1$ the double-humped complex is reflected and for $E > E_2$ transmitted as a whole. Only in between we have partial reflection and transmission as in Fig. 2. Near the discontinuities the percentage of each orbital being located on each side of the density minimum changes smoothly. It is interesting to note that the reflected fragment for $E_1 < E < E_2$ has approximately the thickness of the first "magic" slab (0.38 fm^{-2}). This may indicate some special role played by such "elementary" fragments - at least in 1D-TDHF dynamics.

Fig. 5 shows the energy dependence of the transmission coefficient for slabs of thickness $A = 2.0 \text{ fm}^{-2}$. In each of the three considered cases three discontinuities at different positions are characteristic.

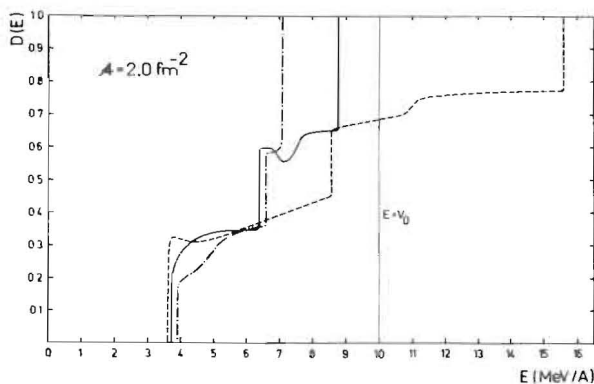


Fig. 5. Energy dependence of the transmission coefficient for the potential (14) from the steep side (dashed line), the flat side (dott-dashed line) and for the corresponding symmetric potential (full line). Slabs with $A = 2.0 \text{ fm}^{-2}$ are considered.

From Fig. 3 we have seen that the origin of this discontinuities in the same as for $A = 1.0 \text{ fm}^{-2}$ slabs: the delicate balance between repulsive external potential and attractive nuclear force "decides" whether a deep minimum formed due to the corresponding appropriate position of the single particle orbitals leads to the transmission of a further fragment or not. In Fig. 3 displaying the origin of the discontinuity of $D(E)$ at $E_2 = 8.6 \text{ MeV}$ it is seen that the fragment additionally transmitted slightly above E_2 is also approximately of the thickness of the first "magic" slab. With increasing energy the number of fragments remains the same while the transmitted ones increase

more or less smoothly in thickness. After the first discontinuity of $D(E)$ one has one, after the second-two, and slightly above the third-three transmitted fragments. At $E \gg E_2$ the slab is transmitted and at $E \ll E_1$ reflected as a whole without being fragmented.

5. Intensified and Asymmetric Penetration

Now we return to the question of whether the asymmetry in the penetrability of asymmetric barriers predicted in ref.^{17/} for an idealized one-dimensional quasideuteron can be seen for a many-particle system in 1D-TDHF. Fig. 5 demonstrates that the effect is really present for most of the energy region where $0 < D < 1$. While for $E > 7.1 \text{ MeV}$ the barrier penetrability is $D = 1$ for approaching the potential from its flat side, the penetrability from the steep side is less than unity up to $E = 15.6 \text{ MeV}$. For $E < 6.6 \text{ MeV}$ the result is opposite to the expectation of ref.^{17/}, i.e., the potential is more penetrable from the steep side. The effect in this energy region is, however, much less pronounced. It is interesting to note, that the penetrability for the corresponding symmetric potential, although mostly lying in between the two values for the asymmetric potential, can turn out to be higher as well as smaller than both values for the asymmetric case in some quite small energy regions.

For smaller slabs and the same potentials the asymmetry effect is less pronounced. So, for $A = 1.0 \text{ fm}^{-2}$ slabs the energy difference of the discontinuities where $D(E)$ reaches unity values for both sides of the potential (14) is nearly the same as $E_2 - E_1$ in Fig. 4. The corresponding values of E_1 nearly coincide. For slabs of thickness $A < 0.80 \text{ fm}^{-2}$ no asymmetry effect could be established (in accordance with a very small amount of excitation). Moreover, for such slabs the penetrability jumps immediately from 0 to 1 at energies somewhat below the barrier height V_0 . That is, thin slabs behave like classical objects. The fact that they penetrate the barrier already at $E \leq V_0$ is probably connected with the finite dimensions of the slab which lower the effective potential felt by them.

Concerning the "intensified tunnelling" considered in refs.^{15,6/} we first consider the question of what to compare our results with. Since for any finite slab thickness in the given geometry the slab consists of an infinite number of nucleons, there is a substantial difference in considering either the single-particle penetrability in the N -th power, i.e., the simultaneous penetration of N independent particles ($N \rightarrow \infty$) or the penetration of a particle of mass $M = mN$, energy $E_N = N \cdot E$ (E - energy per particle) through a potential of height $V_0 = N V_0$. While for $N = 2$ one gets nearly the same result in

both cases (and exactly the same in first order WKB), for $N \rightarrow \infty$ one gets identical zero for any potential at any energy in the former case but a step function for $D(E)$ with discontinuity at $E = V_0$ in the latter case for any potential. This is because for a fixed velocity v the wave number $k = Mv/\hbar$ goes to infinity with $N \rightarrow \infty$, i.e., one has the same situation as if the mass M would be finite and $\hbar \rightarrow 0$ (classical limit).

Hence, we discuss the effect of collective amplification of barrier penetrability by comparing the TDHF results with the classical values $D(E < V_0) \equiv 0$ and $D(E > V_0) \equiv 1$. Then, in nearly all considered cases substantial intensification of penetrability can be established. The only exception is for thick $A = 2.0 \text{ fm}^{-2}$ slabs approaching the potential (14) from the steep side with energies $E > V_0$ (compare Fig. 5). In this case roughly half of the total energy is converted into excitations which are expected to suppress the effect^{5,6/}. It is interesting, however, to note that although in the other cases the excitation energy may amount up to about 40%, penetrability is substantially enlarged. For thin slabs ($A \lesssim 0.8 \text{ fm}^{-2}$) this is seen from the fact that the discontinuity of $D(E)$ lies below V_0 . It comes the closer to V_0 the smaller A . This means that the effect really increases with increasing slab thickness although the amount of excitation energy is also increasing (see above). Fig. 6 displays the A -dependence of the position of the first (i.e., the only, for $A \lesssim 0.8 \text{ fm}^{-2}$) discontinuity of $D(E)$. Since per definition penetrability is intensified for $E > E_1$, provided that $E_1 < V_0$ the above statement is clearly illustrated. The extrapolation of the calculated points in Fig. 6 and the A -dependence of the degree of excitation leads to the conclusion that the effect vanishes for $A \rightarrow 0$.

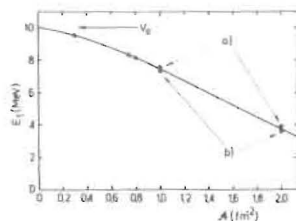


Fig. 6. A -dependence of the position of the first discontinuity of $D(E)$ for the potential (14). The full circles are our numerical results while the full line is drawn to guide the eyes. a) and b) denote the approach of the potential from the flat and steep sides, respectively.

In this limit the slab has no inner structure in Z -direction and behaves like a point-like classical object.

6. Concluding Remarks

Much of the features obtained for slab penetration of external barriers resemble the appearance of soliton-like objects. These are

i) the role of nearly "magic" slabs near the discontinuities of $D(E)$; ii) the classical behaviour of thin slabs (only one orbital occupied) in colliding with the barrier; iii) the relative stability of the shape of such slabs or fragments, and iv) the closeness of their asymptotic velocities to the incident velocity.

Moreover, we have performed numerical calculations for symmetric collisions of "magic" slabs with $A_1 = A_2 = 0.39 \text{ fm}^{-2}$. Even for rather high incident energies ($E_{c.m.} \approx 25 \text{ MeV}$) most of the mass is concentrated in the two final fragments having penetrated each other retaining nearly their initial shapes and velocities. Part of their loss in mass and energy is carried by a small amount of PEP^{13/} and a small piece of matter with central density substantially lower than ρ_0 remaining at rest around $Z=0$.

However, since some amount of excitation is always present, these objects behave like real solitons only asymptotically for $E_{c.m.} \rightarrow 0$ or vanishing external potential in the penetration problem. Then, one has to do with freely translating slabs in its ground state, which are known to be solutions of the TDHF equations (9).

Another interesting observation on this line is that in high-energetic slab collisions fragmentation occurs into exactly as much fragments as orbitals are occupied initially^{8,13/}. Each such final fragment consists of components of all orbitals.

It is possible that the appearance of soliton-like components in the considered 1D-TDHF problems is an artifact of considering a one-dimensional problem, since it is known that the transition to more dimensions can suppress the existence of stable solitary solutions.

A second remark concerns the "classical" definition of $D(E)$ via eq. (16) which was necessary due to some consequences of nonlinearity and, hence, some classical features of the TDHF initial value problem. Recently, several methods have been worked out to approximately quantize the mean-field theory (see ref.^{9/} and references cited therein). For example, quantum fluctuations around the "classical" TDHF "trajectory" in the class of determinantal wave functions can be taken into account using path integral methods. The point is that on this line any observable quantity is also influenced by "trajectories" in the vicinity of that with the least action (only the latter is considered in standard TDHF). They may have discontinuities of $D(E)$ at slightly different positions, so that in a re-

quantized version of TDHF the discontinuities could be smoothed out. Unfortunately, these methods are still far from practical applicability.

The appearance of discontinuities in the energy dependence of $D(E)$ was also obtained in the classical limit in the framework of the coupled channel method^{/14/}. Without channel coupling one has a classical one-step function for $D(E)$. Taking into account N coupled channels, the classical limit yields a N -step function for $D(E)$. Quantum effects lead to a smoothing out of the discontinuities.

From these remarks we conclude that the appearance of step-like discontinuities in our 1D-TDHF results is one more classical feature of the TDHF theory. Independently on whether they would exist also in 3 dimensions they should be smeared out if taking into account quantum fluctuations. We claim, however, that this would not change our qualitative results on intensified and asymmetric barrier penetration, since it is quite unlikely that quantum fluctuations would also shift the shapes of $D(E)$ in energy and relation to each other for approaching the potential from the steep or flat side.

So, we claim that the effects predicted in ref.^{/5-7/} for very simple situations could be demonstrated to exist also in a more involved many-particle treatment.

References

1. Revokatova I.P., Zilin A.P. Uspechi Fiz.Nauk, 1984, 142, p. 159.
2. Dittrich J., Exner P. JINR, E2-84-352 and E2-84-383, Dubna, 1984.
3. Lapidus R. Am.J.Phys., 1982, 5, p. 663.
4. Mayer-Vernet N. Am.J.Phys., 1982, 50, p. 353.
5. Zakhariev B.N., Sokolov S.N. Ann. der Physik, 1964, 14, p. 229.
6. Zakhariev B.N. Izv.A.N.SSSR, ser. fiz., 1983, 47, p. 859.
7. Amirkhanov I., Zakhariev B.N. J.Exp.Theor.Phys. (USSR), 1965, 49, p. 1097.
8. Bonche P., Koonin S.E., Negele J.W. Phys.Rev., 1976, C13, p. 1226.
9. Negele J.W. Rev.Mod.Phys., 1982, 54, p. 913.
10. Mädlер P. Particles and Nuclei, 1984, 15, p. 418.
11. Ring P., Schuck P. The Nuclear Many-Body Problem, Springer, N.Y., 1980.
12. Barz B.I. et al. The Hartree-Fock Method in Nuclear Theory (in Russian), Naukova Dumka, Kiev, 1982.
13. Mädlер P. JINR E7-84-85, Dubna, 1984, to appear in Z.Phys. A.
14. Dasso C.H., Landowne S., Winther A. Nucl.Phys., 1983, A405, p. 381; A407, p. 221.

Received by Publishing Department
on July, 10 1984.

Мэдлер П., Никишов П.Ю., Захарьев Б.Н.
Усиление и асимметрия проницаемости барьера

E4-84-487

для ядерных слоев в приближении зависящего от времени Хартри-Фока

Эффекты усиления и нарушения симметрии проницаемости барьеров сложными частицами, обладающими внутренними степенями свободы, исследуются в рамках зависящего от времени среднего поля с использованием эффективной одномерной геометрии слоев и упрощенных эффективных сил Скинра между нуклонами. Коэффициент проницаемости $D(E)$ вычислен как функция энергии налетающего на барьер слоя и его толщины. Детально обсуждается наличие скачков в поведении $D(E)$. Есть основания предполагать, что квантовые поправки к стандартной ХФВ-картине, как и увеличение размерности, приведет к сглаживанию скачков, но не изменит качественных результатов. Они заключаются в том, что во всех рассмотренных случаях проницаемость, действительно, существенно усиливается и имеет место эффект асимметрии, как предсказывалось ранее на основе простой квазидейтронной модели.

Работа выполнена в Лаборатории теоретической физики ОИЯИ.

Сообщение Объединенного института ядерных исследований. Дубна 1984

Mädler P., Nikishov P.Yu., Zakhariev B.N.
Intensified and Asymmetric Barrier Penetration
of Nuclear Slabs In TDHF Approximation

E4-84-487

The effects of intensified and asymmetric barrier penetration by complex particles exhibiting intrinsic structure are investigated in the framework of the time-dependent mean-field theory using an effective one-dimensional slab geometry and a simplified Skyrme nucleon-nucleon effective interaction. The transmission coefficient $D(E)$ has been investigated as a function of incident energy E and slab thickness. The appearance of discontinuities in $D(E)$ is discussed in detail. It is argued that quantum corrections to the standard TDHF picture as well as the transition to three dimensions possibly smearing out the discontinuities should not alter the qualitative results. In nearly all considered cases the penetrability is really substantially intensified and the asymmetry effect manifests itself as predicted earlier using a simple quasideuteron model.

The investigation has been performed at the Laboratory of Theoretical Physics, JINR.

Communication of the Joint Institute for Nuclear Research, Dubna 1984